Cell Reports

NS5A Promotes Constitutive Degradation of IP3R3 to Counteract Apoptosis Induced by Hepatitis C Virus

Graphical Abstract

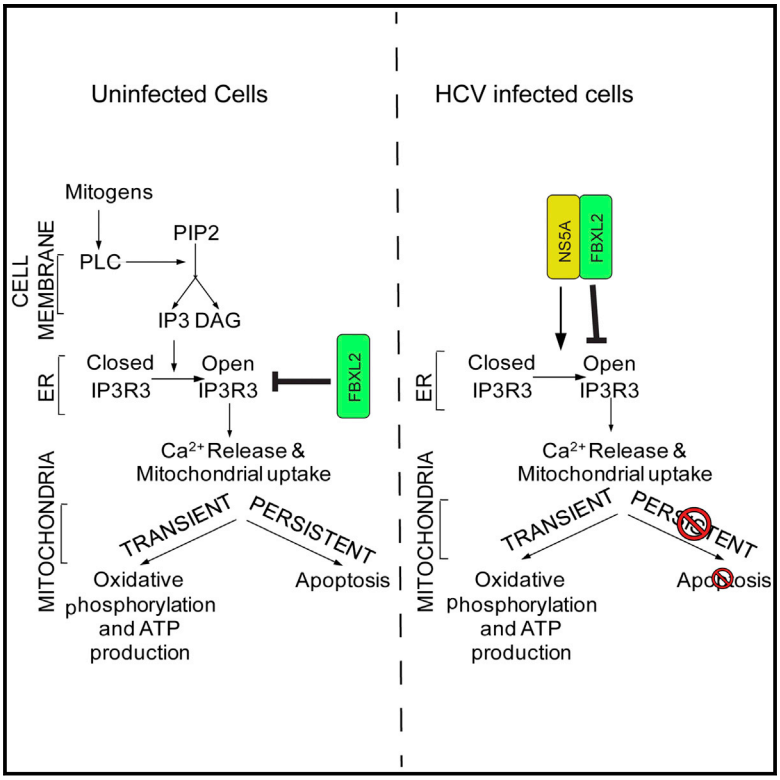

Highlights

- NS5A unmasks the IP3R3 degron to promote its FBXL2-dependent degradation
- Constitutive IP3R3 degradation inhibits calcium flux and, consequently, viral-induced apoptosis
- Inhibition of HCV replication upon FBXL2 silencing is rescued by IP3R3 co-depletion
- Pharmacologic inhibition of either FBXL2 or NS5 localization inhibits HCV replication

Authors

Shafi Kuchay, Mohsan Saeed, Carlotta Giorgi, ..., Paolo Pinton, Charles M. Rice, Michele Pagano

Correspondence

kuchay@uic.edu (S.K.), ricec@mail.rockefeller.edu (C.M.R.), michele.pagano@nyumc.org (M.P.)

In Brief

Kuchay et al. show that the HCV NS5A protein forms a complex with IP3R3 and FBXL2 and promotes constitutive FBXL2-mediated degradation of IP3R3. IP3R3 degradation inhibits calcium flux, mitochondrial calcium overload, and apoptosis. Thus, NS5A contributes to a cellular environment that is permissive for chronic HCV infection.

Kuchay et al., 2018, Cell Reports *25*, 833–840
October 23, 2018
https://doi.org/10.1016/j.celrep.2018.09.088

CellPress

Cell Reports
Report

NS5A Promotes Constitutive Degradation of IP3R3 to Counteract Apoptosis Induced by Hepatitis C Virus

Shafi Kuchay,[1,2,5,6,*] Mohsan Saeed,[3,5] Carlotta Giorgi,[1,4] Jie Li,[1] Hans-Heinrich Hoffmann,[3] Paolo Pinton,[4] Charles M. Rice,[3,*] and Michele Pagano[1,2,7,*]

[1]Department of Biochemistry and Molecular Pharmacology, Laura and Isaac Perlmutter NYU Cancer Center, New York University School of Medicine, 522 First Avenue, SRB 1107, New York, NY 10016, USA

[2]Howard Hughes Medical Institute, 522 First Avenue, SRB 1107, New York, NY 10016, USA

[3]Laboratory of Virology and Infectious Disease, Center for the Study of Hepatitis C, The Rockefeller University, New York, NY 10065, USA

[4]Department of Morphology, Surgery and Experimental Medicine, Section of Pathology, Oncology and Experimental Biology, Laboratory for Technologies of Advanced Therapies (LTTA), University of Ferrara, Ferrara, Italy

[5]These authors contributed equally

[6]Present address: Department of Biochemistry and Molecular Genetics, University of Illinois College of Medicine at Chicago, 900 S. Ashland Avenue, #1252, Chicago, IL 60607, USA

[7]Lead Contact

*Correspondence: kuchay@uic.edu (S.K.), ricec@mail.rockefeller.edu (C.M.R.), michele.pagano@nyumc.org (M.P.)

https://doi.org/10.1016/j.celrep.2018.09.088

SUMMARY

FBXL2 targets IP3R3 for ubiquitin-mediated degradation to limit Ca^{2+} flux to mitochondria and, consequently, apoptosis. Efficient replication of hepatitis C virus (HCV) requires geranylgeranylation of FBXL2. Here, we show that the viral protein NS5A forms a trimeric complex with IP3R3 and FBXL2, unmasking IP3R3's degron in the absence of inositol 1,4,5-trisphosphate (IP_3) stimulation. FBXL2 knockdown or expression of a stable IP3R3 mutant causes persistent Ca^{2+} flux and sensitizes cells to apoptosis, resulting in the inhibition of viral replication. Importantly, the effect of FBXL2 silencing is rescued by depleting IP3R3, but not p85β, another established FBXL2 substrate, indicating that the anti-HCV effect of FBXL2 knockdown is largely due to IP3R3 stabilization. Finally, disruption of the FBXL2-NS5A-IP3R3 complex using somatic cell genetics or pharmacologic inhibition results in IP3R3 stabilization and suppression of HCV replication. This study reveals an IP_3-independent molecular mechanism through which HCV promotes IP3R3 degradation, thereby inhibiting virus-induced apoptosis and establishing chronic infection.

INTRODUCTION

FBXL2 is a member of the family of F-box proteins (Kuchay et al., 2013, 2017), which are substrate-targeting subunits for SCF (SKP1, CUL1, F-box protein) ubiquitin ligase complexes (Skaar et al., 2013). In humans, there are 69 SCF ligases, each utilizing a different F-box protein subunit (Skaar et al., 2009). FBXL2 contains a COOH-terminal CaaX domain that is required for its geranylgeranylation and localization at cell membranes (Kuchay et al., 2013, 2017; Wang et al., 2005). So far, two cellular substrates of FBXL2 have been shown to be localized on cellular membranes and require FBXL2 geranylgeranylation for their degradation: p85β (one of the regulatory subunits of PI3K) and IP3R3 (see below; Kuchay et al., 2013, 2017).

FBXL2, in its geranygeranylated form, is required for efficient hepatitis C virus (HCV) replication (Wang et al., 2005). HCV is a plus-stranded RNA virus, whose genome encodes a single polyprotein that is processed by viral and host proteases to yield three structural (core, E1, and E2) and seven non-structural (p7, NS2, NS3, NS4A, NS4B, NS5A, and NS5B) proteins (Lindenbach and Rice, 2005). HCV NS3/4A protease, NS5B RNA polymerase, and NS5A protein are the major targets of interferon-free direct-acting antiviral regimens, some of which are showing remarkable clinical benefits (Bourlière et al., 2017). FBXL2 physically interacts with NS5A (Wang et al., 2005), the viral protein that localizes to the cytoplasmic and/or perinuclear cellular compartment containing the endoplasmic reticulum (ER) and the Golgi apparatus (Lindenbach and Rice, 2005; Wang et al., 2005). However, the molecular mechanism that makes FBXL2 critical for viral replication has remained unknown.

Despite lacking any overt enzymatic activity, NS5A is a key modulator of HCV pathogenesis. NS5A is a phosphoprotein involved in several HCV functions, ranging from modulating the host immune response to having a direct role in HCV RNA replication. Importantly, NS5A prevents apoptosis of infected cells, permitting longer periods of viral replication and contributing to virus persistence (Lindenbach and Rice, 2005). However, the molecular mechanisms by which NS5A inhibits apoptosis are not completely understood. Furthermore, NS5A is the target of BMS-790052 (daclatasvir), a DAA approved for interferon-free, oral regimens in patients with chronic hepatitis C (Rice and Saeed, 2014).

Inositol 1,4,5-trisphosphate (IP_3) receptors (IP3Rs) form tetrameric channels that open upon binding to IP_3 to release calcium (Ca^{2+}) from the ER, the major intracellular store of Ca^{2+} (Kuchay et al., 2017). The three mammalian IP3Rs display differential

tissue and developmental expression, and their subcellular localizations are not completely overlapping. Specifically, IP3R3 is enriched in the mitochondrial-associated membrane (MAM) regions, where the ER exchanges Ca^{2+} ions with mitochondria (Giorgi et al., 2009). In response to stimuli that promote IP_3 generation (e.g., growth factors, hormones, and neurotransmitters that activate phospholipase C), IP3R3 induces transient Ca^{2+} mobilization from the ER to mitochondria. IP_3-induced mitochondrial uptake of Ca^{2+} is necessary for oxidative phosphorylation and ATP production. However, persistent Ca^{2+} release results in mitochondrial Ca^{2+} overload, opening of the permeability transition pore, release of caspase cofactors, and apoptosis (Mattson and Chan, 2003; Orrenius et al., 2003). Thus, the duration and extent of the Ca^{2+} mobilization determines whether cells survive or die. IP3R3 appears to be the major player in the pro-apoptotic transfer of Ca^{2+} from the ER to mitochondria (Giorgi et al., 2012). Accordingly, downregulation of IP3R3 inhibits Ca^{2+}-mediated apoptosis (Blackshaw et al., 2000).

We have shown that the SCF^{FBXL2} ubiquitin ligase targets IP3R3 for degradation to avoid an excessive and prolonged flux of Ca^{2+} and attenuate apoptosis in response to Ca^{2+}-dependent stress (Kuchay et al., 2017). This process requires the presence of FBXL2 at cell membranes via geranylgeranylation and is therefore sensitive to geranylgeranylation inhibitors, some of which have reached clinical trials. Here, we show that N55A, by unmasking the IP3R3 degron for FBXL2 recognition, promotes FBXL2-mediated degradation of IP3R3 and thereby counteracts HCV-induced apoptosis.

RESULTS

NS5A Unmasks the IP3R3 Degron to Promote FBXL2 Recognition

Inhibition of protein geranylgeranylation prevents HCV RNA replication (Kapadia and Chisari, 2005; Ye et al., 2003); however, the absence of canonical prenylation motifs in HCV-encoded proteins suggests that one or more host geranylgeranylated proteins are required for HCV RNA replication. In a screen to identify these host cell protein(s), FBXL2 was identified and shown to physically interact with NS5A (Wang et al., 2005). We confirmed that FBXL2, but not FBXL2(CaaX/SaaX), a geranylgeranylation-deficient mutant that does not localize to cell membranes and does not bind active, neddylated CUL1 (Kuchay et al., 2017; Wang et al., 2005), binds NS5A protein from all HCV genotypes tested (genotypes 1a, 1b, 2a, 3a, and 4a; Figure 1A). Accordingly, endogenous FBXL2 interacted with NS5A in HCV-infected Huh-7.5 cells (Figure S1A).

Addition of serum to serum-starved cells promotes IP3R3 degradation (Kuchay et al., 2017). We used HepG2, a liver cancer cell line that is sensitive to serum, and found that the expression of increasing amounts of NS5A enhanced the serum-stimulated degradation of IP3R3 (Figure 1B), decreased Ca^{2+} mobilization from the ER to the mitochondria (Figure 1C), and protected cells from apoptosis, as shown by a decrease in cleaved PARP and cleaved caspase 3 (Figure 1B; see also Figure 3C). NS5A acted through FBXL2 because FBXL2 silencing abolished NS5A's effects on IP3R3 degradation, apoptosis, and cell survival. These effects were particularly evident when cells were treated with H_20_2 that induces oxidative stress, leading to Ca^{2+}-mediated apoptosis (Figures 1D and S1B). Expression of increasing amounts of NS5A proportionally enhanced the binding of FBXL2 to IP3R3, and *vice versa*, exogenous FBXL2 increased the interaction between NS5A and IP3R3 (Figure 1E). Finally, infection of Huh7.5 cells with Jc1-HCV virus promoted the ubiquitylation of IP3R3 (Figure S1C). This was observed by expressing a FLAG-tagged trypsin-resistant tandem ubiquitin-binding entity (TR-TUBE), which directly binds poly-ubiquitin chains and protects them from proteasome-mediated degradation (Dankert et al., 2016). After immunoprecipitation of FLAG-tagged TR-TUBE, high-molecular-weight ubiquitylated species of IP3R3 were detected more abundantly in lysates of infected cells than non-infected cells (Figure S1C).

IP_3 binding evokes conformational changes that open the suppressor domain of IP3R3 (Fan et al., 2015). We found that FBXL2 binds IP3R3 upon IP_3 production (Kuchay et al., 2017), indicating that the suppressor domain of IP3R3 (amino acids 1–226) masks the IP3R3's degron (i.e., the amino acid region required for binding to and degradation via FBXL2). To understand the basis for NS5A-mediated effects, we mapped the NS5A-binding domain in IP3R3 and found that NS5A binds the first 602 amino acids (Figure S1D). Because this truncation mutant does not efficiently bind FBXL2 unless IP_3 production is induced (Kuchay et al., 2017), it appears that FBXL2 is not necessary to bridge IP3R3 to NS5A. Accordingly, IP3R3(Q-FR/A-AA), which does not bind FBXL2 (Kuchay et al., 2017) is still able to co-immunoprecipitate with NS5A, although to a lesser extent compared to wild-type IP3R3 (Figure S1E). This suggests that, although FBXL2 is not required for NS5A-IP3R3 interaction, its presence may stabilize the protein complex.

We then expressed tagged constructs of NS5A, FBXL2, and IP3R3 in HEK293T cells and performed immunoprecipitation experiments. As expected, FLAG-tagged NS5A co-immunopurified both hemagglutinin (HA)-tagged FBXL2 and GFP-tagged IP3R3 (Figure S1F). When anti-FLAG immunoprecipitates were further precipitated with an anti-GFP antibody and tested for the presence of NS5A, FBXL2, and IP3R3, all three proteins could be detected (Figure S1F), indicating formation of a trimeric complex. Significantly, expression of NS5A in HEK293T cells strongly increased the binding of IP3R3(1–602) to FBXL2 (Figure 2A, top panel, lanes 1–4) and increased IP3R3(1–602) degradation (Figure 2A, third panel from the top, lanes 1–4). In contrast, IP3R3(227–602), which does not contain the N-terminal suppressor domain (and therefore binds FBXL2, even in the absence of IP_3 production), was unaffected by NS5A expression (Figure 2A, lanes 5–8). Finally, expression of increasing amounts of NS5A decreased the levels of wild-type IP3R3, but not the levels of the IP3R3(Q-FR/A-AA) stable mutant (Figure 2B), which does not bind FBXL2 (Kuchay et al., 2017). Similarly, increasing the expression of NS5A resulted in a decrease in Ca^{2+} mobilization from the ER to the mitochondria in cells expressing wild-type IP3R3, but not IP3R3(Q-FR/A-AA) (Figure 2C).

These results, together with the finding that the N-terminal suppressor domain masks the IP3R3 degron (Kuchay et al., 2017), suggest that NS5A promotes the IP3R3-FBXL2

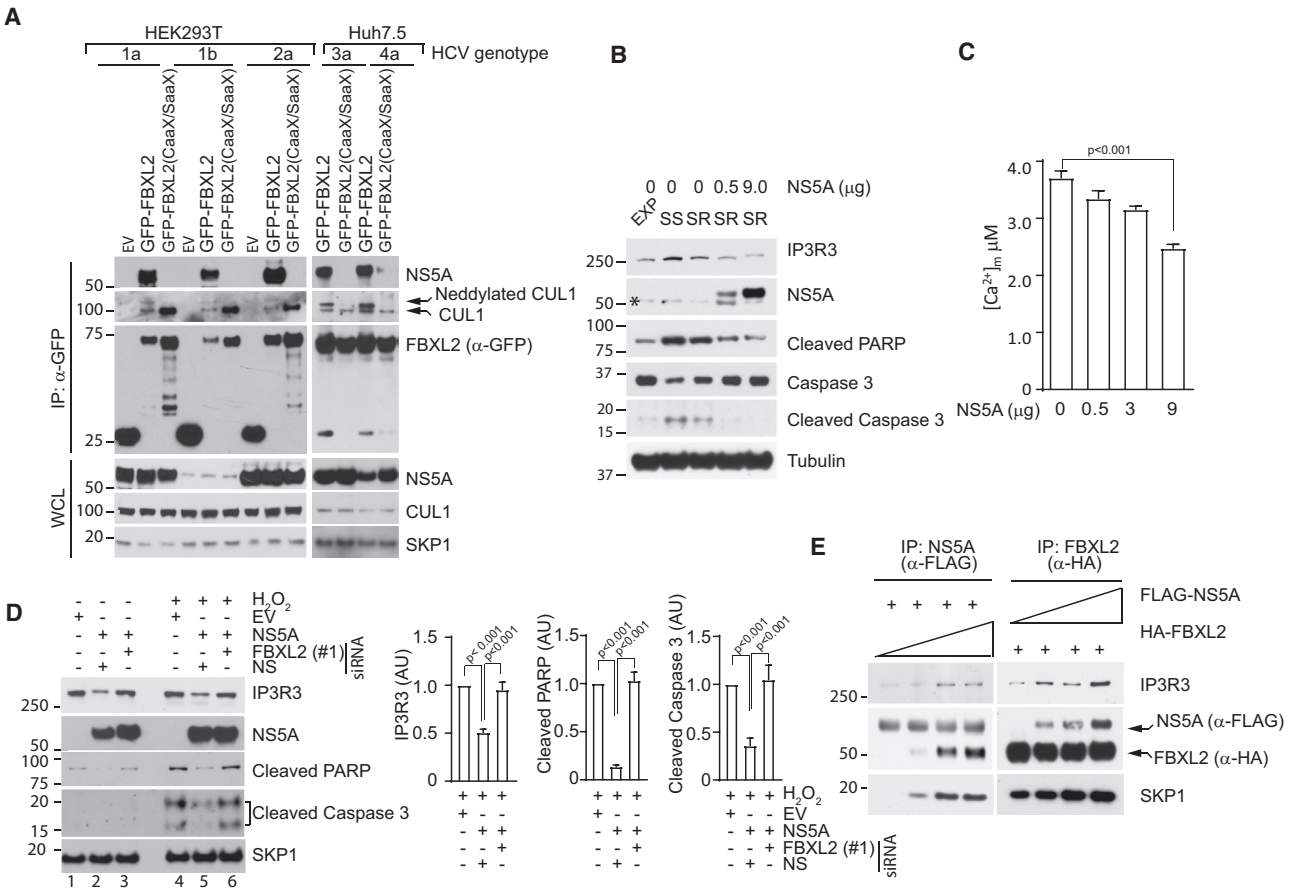

Figure 1. NS5A Promotes IP3R3-FBXL2 Interaction and IP3R3 Degradation and Inhibits Ca^{2+} Flux

(A) HEK293T or Huh7.5 cells expressing NS5A from the indicated HCV genotypes were transfected with either empty vector (EV), GFP-FBXL2, or GFP-FBXL2(CaaX/SaaX) plasmids. Sixteen hours post-transfection, cells were treated with MG132 for three hours prior to harvesting for immunoprecipitations and immunoblotting as indicated. WCL, whole-cell lysate.

(B) Exponentially growing (EXP) HepG2 cells were transfected with the indicated amounts of NS5A cDNA, serum starved for 24 hr (SS), and then re-stimulated with serum for one hour (SR) prior to cell lysis and immunoblotting. The asterisk indicates a non-specific band.

(C) The experiment was performed as in (A), except that, after re-stimulation, cells were treated with a purinergic G-protein coupled receptor (GPCR) agonist (ATP) and concentration of mitochondrial Ca^{2+} was measured. Graphs show quantification from four independent experiments, each performed at least in duplicate.

(D) HepG2 cells were transfected with either a small interfering RNA (siRNA) targeting FBXL2 or a non-silencing siRNA (NS) for 48 hr and then an EV or NS5A cDNA for 16 hr. Cells were treated with vehicle or H_2O_2 for 10 hr, and cell extracts were processed for immunoblotting. The bar graphs show the quantification of IP3R3 and cleaved forms of PARP and caspase 3 from three independent experiments, represented as fold change (a.u.) compared to lane 4, which was set as 1.0. p values were calculated by a one-way ANOVA and multiple-comparisons test. Error bars indicate SEM.

(E) HEK293T cells were co-transfected with FLAG-NS5A and increasing amounts of HA-FBXL2 (left panels) or with HA-FBXL2 and increasing amounts of FLAG-NS5A (right panels). Twenty-four hours post-transfection, cells were treated with MG132 for three hours prior to immunoblotting.

interaction by forming a trimeric complex that displaces the IP3R3 suppressor domain and unmasks the IP3R3 degron for FBXL2 recognition, thereby promoting IP3R3 degradation in the absence of IP_3 induction.

FBXL2 Promotes HCV Infection by Targeting IP3R3 for Degradation

Silencing of FBXL2 inhibits replication of an HCV replicon (genotype 1b) in Huh7-HP cells (Wang et al., 2005). We confirmed these results in Huh7.5-JFH1 and Huh7.5-Con1 cells, two cell lines harboring persistently replicating HCV subgenomic replicons from genotype 2a (JFH1/SG-Feo) and genotype 1b (Con1/SG-Feo S2204I), respectively (Figures 3A and S2A). Knockdown of FBXL2 in the replicon cells led to an approximately 50% decrease in replication.

To determine whether this effect was dependent on the stabilization of IP3R3, we silenced FBXL2 in combination with either IP3R3 or p85β, another substrate of FBXL2 (Kuchay et al., 2013). When IP3R3 and FBXL2 were silenced together, HCV replication levels returned to those detected in control cells (Figures 3A and S2A). In contrast, no substantial differences in replication were observed when either p85β (alone or in combination with FBXL2) or IP3R3 alone were silenced.

To evaluate whether IP3R3-mediated Ca^{2+} flux plays a role in viral replication, we used two different strategies: (1) we co-depleted MCUa in FBXL2 knockdown cells to inhibit

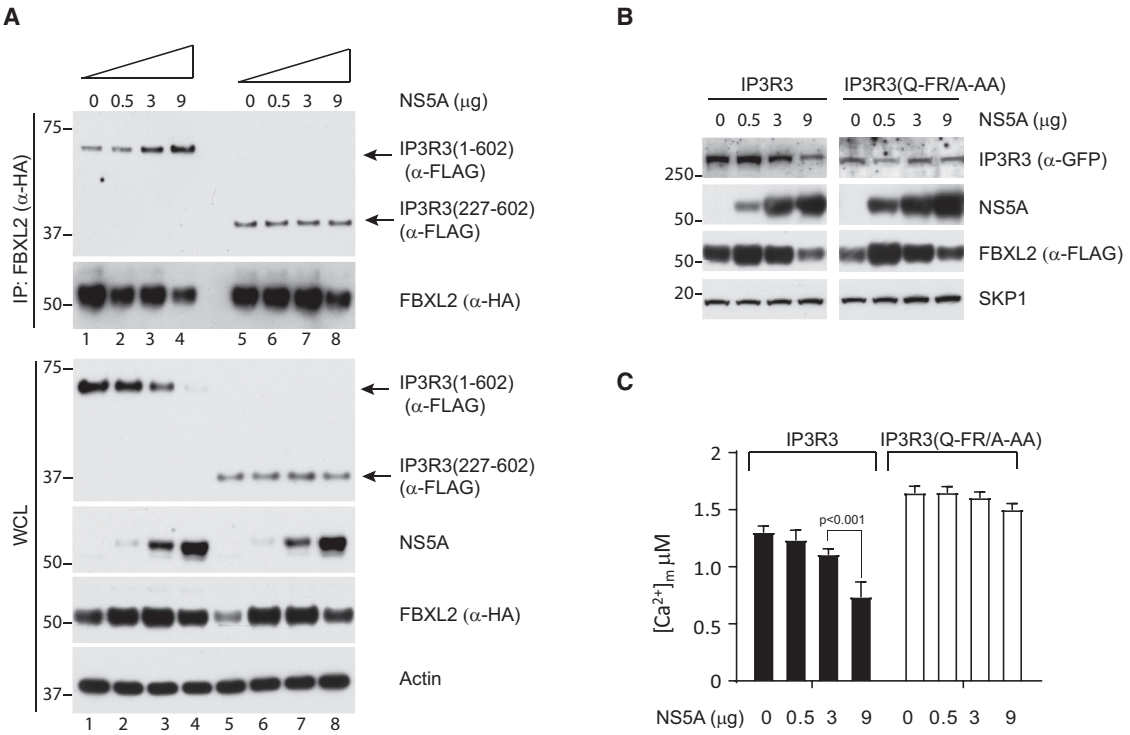

Figure 2. NS5A Unmasks the IP3R3 Degron

(A) HEK293T cells were co-transfected with HA-FBXL2 and increasing amounts of NS5A cDNA, together with either FLAG-IP3R3(1–602) or FLAG-IP3R3(227–602). Twenty-four hours post-transfection, cells were harvested for immunoprecipitations and immunoblotting.

(B) COS-7 cells were co-transfected with FLAG-FBXL2 and increasing amounts of NS5A cDNA, together with either GFP-IP3R3 or GFP-IP3R3(Q-FR/A-AA). Twenty-four hours post-transfection, cells were harvested for immunoblotting.

(C) The experiment was performed as in (B), except that cells were treated with ATP and concentration of mitochondrial Ca^{2+} was measured and analyzed by two-way ANOVA multiple-comparisons test in three independent experiments, each performed at least in duplicate.

mitochondrial Ca^{2+} overload (and, consequently, Ca^{2+}-mediated apoptosis) and (2) we treated FBXL2 knockdown cells with cyclosporin A (CsA) to inhibit the opening of the mitochondrial permeability transition pore and Ca^{2+}-dependent apoptosis. We observed that both strategies counteracted the inhibition of HCV replication induced by FBXL2 silencing (Figure S2B). Accordingly, FBXL2 depletion in Huh7.5-JFH1 and Huh7.5-Con1 cells increased Ca^{2+} flux from ER to mitochondria, and this effect was rescued by co-depletion of IP3R3 (Figure S2C). Finally, silencing of FBXL2 in Huh7.5-JFH1 cells decreased cell viability and promoted apoptosis, two phenotypes that were rescued by co-silencing IP3R3 (Figures S2D and S2E).

In agreement with the above results, expression of IP3R3(Q-FR/A-AA) or, to a lesser extent, wild-type IP3R3 significantly reduced viral replication in Huh7.5-JFH1 and Huh7.5-Con1 cells (Figure 3B, upper panels), with simultaneous induction of apoptosis, as assessed by the cleavage of caspase 3 and TUNEL assay (Figure 3B, middle and lower panels), and an increase in $[Ca^{2+}]_m$ (Figure S2F).

Together, these results suggest that FBXL2 promotes HCV replication largely by mediating IP3R3 degradation, thereby preventing mitochondrial Ca^{2+} overload and subsequent apoptosis.

We further validated these findings in the context of the complete HCV life cycle. HCV infection of Huh-7.5 cells induced apoptosis, as evidenced by the appearance of cleaved PARP and caspase 3 (Figures 3C, S2G, and S2H). Depletion of FBXL2 decreased HCV replication, stabilized IP3R3, and exacerbated virus-induced apoptosis (Figures 3C, S2G, and S2H). Importantly co-silencing of IP3R3 partially reversed the effects of FBXL2 depletion (Figure 3C).

Disruption of NS5A-FBXL2-IP3R3 Trimeric Complex Inhibits HCV Replication

FBXL2 has to be geranylgeranylated for its activity (Kuchay et al., 2013, 2017). Inhibition of FBXL2 geranylgeranylation using a geranylgeranyl transferase inhibitor causes an increase in IP3R3 level, mitochondrial Ca^{2+} overload, and a decrease in cell viability (Kuchay et al., 2017). Because FBXL2 knockdown inhibited HCV replication by stabilizing IP3R3 (Figure 3A), we asked whether geranylgeranylation inhibitors also inhibit HCV replication by the same mechanism. If this is the case, then IP3R3 knockdown should overcome the effects of geranylgeranylation inhibitors on HCV replication. To this end, we treated Huh7.5-JFH1 cells with increasing amounts of a geranylgeranyl transferase inhibitor (GGTi-286). This treatment inhibited HCV RNA replication in a dose- and time-dependent manner, and remarkably, IP3R3 silencing significantly counteracted this inhibition (Figure 4A).

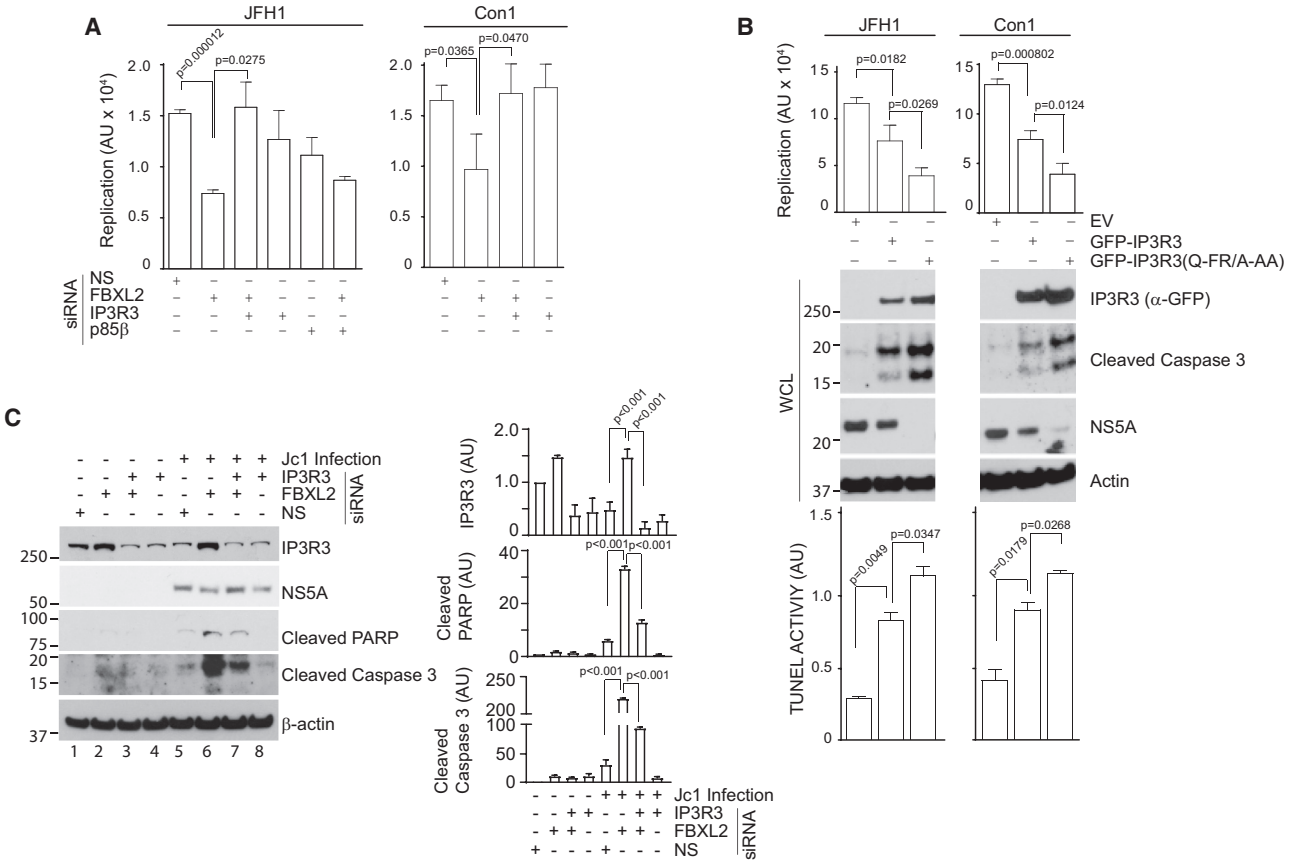

Figure 3. Failure to Degrade IP3R3 Inhibits HCV Replication

(A) Huh7.5-JFH1 and Huh7.5-Con1 cells were transfected twice with the indicated siRNAs and firefly luciferase activity measured 48 hr after to quantify HCV replication. Plotted are the means ± SEM of three independent experiments. Statistical analysis was performed with t tests and ANOVA using Graphpad prism software.

(B) Huh7.5-JFH1 and Huh7.5-Con1 cells were transfected with GFP-tagged IP3R3 or IP3R3(Q-FR/A-AA) for 64 hr. Then, luciferase activity was measured to quantify HCV replication (top graphs), cell lysates analyzed by immunoblotting (middle panels), and TUNEL assay performed to quantify apoptosis (bottom graphs). Graphs show means ± SEM of three independent experiments (top) and two independent experiments (bottom). Statistical analysis was performed with t tests and ANOVA using Graphpad prism software.

(C) Huh7.5 cells were transfected twice with the indicated siRNAs. Twenty-four hours after, cells were infected with Jc1FLAG2(p7-nsGLuc2A), a highly infectious HCVcc virus. Four hours post-infection, cells were washed with PBS and fresh medium, collected, and analyzed by immunoblotting. The bar graphs show the quantification of IP3R3 and cleaved forms of PARP and caspase 3 levels from three independent experiments, represented as fold change (a.u.) compared to lane 1, which was set as 1.0. p values were calculated by a one-way ANOVA and multiple-comparisons test. Error bars indicate SEM.

We further explored the molecular mechanism by which GGTI-286 affects the FBXL2-NS5A complex and found that GGTI-286 treatment completely inhibited the binding of FBXL2 to NS5A (Figure 4B, lanes 1 versus 2). Moreover, FBXL2(CaaX/SaaX), which does not localize to cell membranes (Kuchay et al., 2013; Wang et al., 2005), did not interact with either IP3R3 (Kuchay et al., 2017) or NS5A (Figure 4B, lane 4). Thus, if FBXL2 is not properly localized in the cell, it is unable to interact with NS5A and IP3R3. We reasoned that IP3R3 at cell membranes might help bridging FBXL2 and NS5A. To test this hypothesis, we utilized IP3R3(1–602), an IP3R3 deletion mutant that cannot be anchored to membranes. Despite the presence of GGTI-286, expression of IP3R3(1–602) promoted the binding of both wild-type FBXL2 and FBXL2(CaaX/SaaX) to NS5A (Figure 4B, lanes 3 and 5). This result indicates that IP3R3 bridges NS5A and FBXL2, in agreement with its ability to form a trimeric complex with these proteins (Figure S1F), and suggests that the trimeric complex requires all three proteins to be in the same compartment. In the presence of GGTi-286, FBXL2 and NS5A are not stably anchored to cell membranes where endogenous IP3R3 is localized, but expression of a "mobile" IP3R3(1–602) mutant re-allows trimeric complex formation.

Taken together, these results suggest that GGTi-286 suppresses HCV infection by inhibiting FBXL2 geranylgeranylation and localization and, consequently, its interaction with IP3R3.

We then sought to block NS5A membrane localization and examine its effects on NS5A-FBXL2-IP3R3 interaction. To this end, we used BMS-790052 (daclatasvir), a powerful anti-HCV drug that has been shown to change NS5A localization from ER membranes to lipid droplets (Liu et al., 2015). Thus,

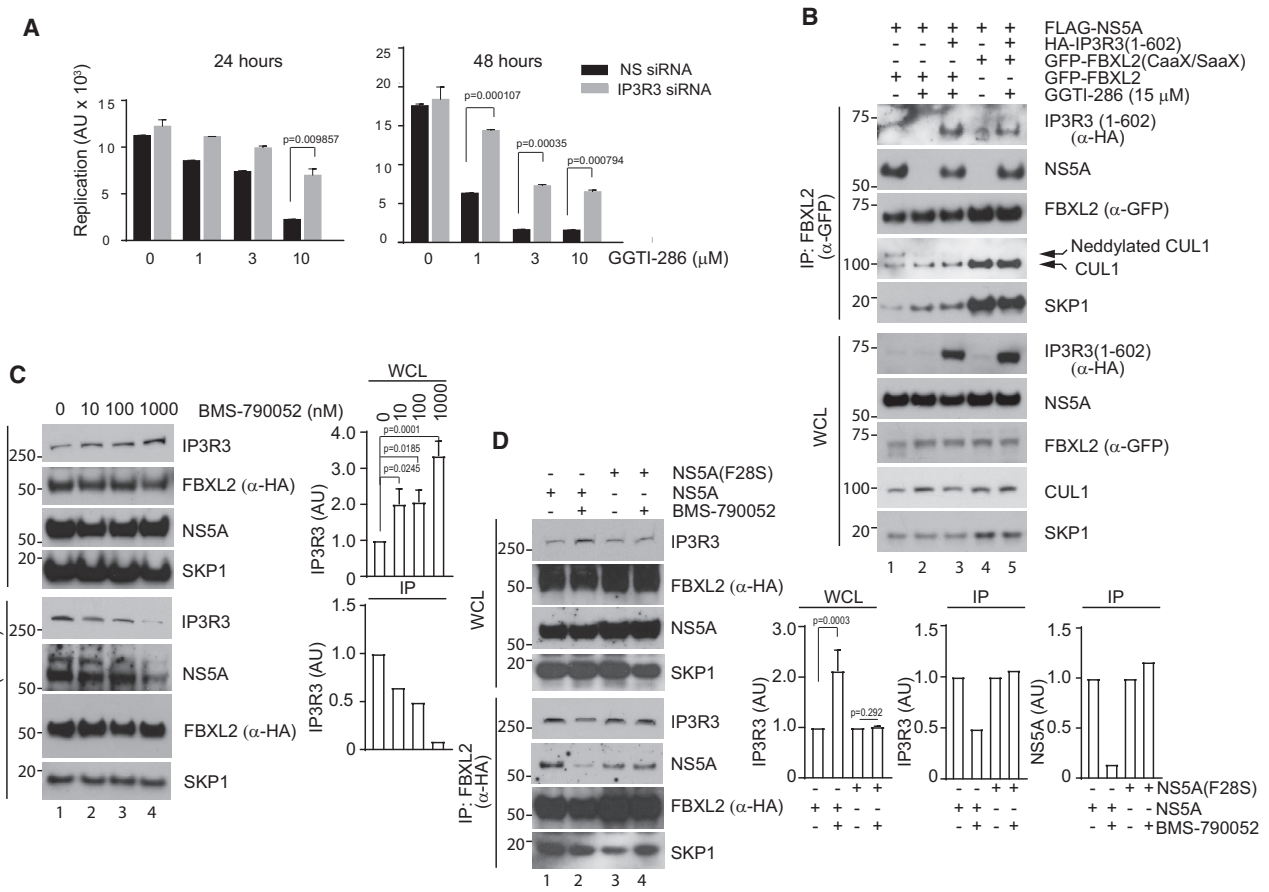

Figure 4. GGTI-286 and BMS-790052 Inhibit NS5A Binding to FBXL2 and HCV Replication

(A) Huh7.5-JFH1 cells were transfected twice with the indicated siRNAs. Twenty-four hours after, cells were trypsinized and re-plated in fresh medium. The next day, cells were treated for 24 or 48 hr with either vehicle (DMSO) or the indicated concentrations of GGT1-286, after which cells were lysed and firefly luciferase activity measured. Graphs show means ± SEM of two experiments, each performed in duplicate. Statistical analysis was performed with t tests using Graphpad prism software.

(B) HEK293T cells were transfected with the indicated cDNAs. Where indicated, 15 μM GGTI-286 was added for 20 hr before harvesting. WCLs were immunoprecipitated and immunoblotted.

(C) Huh7.5-JFH1 cells stably expressing HA-FBXL2 were treated with the indicated concentrations of BMS-790052 for 8 hr before harvesting for immunoprecipitations and immunoblotting. The graphs show the quantification of IP3R3 levels analyzed by a one-way ANOVA and multiple-comparisons test, represented as fold change (a.u.) compared to lane 1, which was set as 1.0. Three independent experiments were quantified for whole-cell extracts, and two independent experiments were quantified for immunoprecipitates. Error bars indicate SEM.

(D) Huh7.5 cells infected with either the wild-type Jc1FLAG2(p7-nsGLuc2A) virus or a BMS-790052-resistant Jc1FLAG2(p7-nsGLuc2A) variant were transfected with HA-FBXL2 and treated with BMS-790052 for 8 hr before harvesting for immunoprecipitations and immunoblotting. The graphs show the quantification of IP3R3 and NS5A levels analyzed by a one-way ANOVA and multiple-comparisons test, represented as fold change (a.u.) compared to lane 1, which was set as 1.0. Three independent experiments were quantified for whole-cell extracts, and two independent experiments were quantified for immunoprecipitates. Error bars indicate SEM.

we examined the effect of BMS-790052 on NS5A binding to FBXL2 in Huh7.5-JFH1 cells stably expressing FBXL2 under the control of a weak retroviral promoter. BMS-790052 induced IP3R3 accumulation in a dose-dependent manner (Figure 4C, top panel). Interestingly, despite increased IP3R3 levels, the binding of FBXL2 to IP3R3 as well as to NS5A was inhibited by BMS-790052 (Figure 4C, bottom panel). Similar results were obtained in cells transiently expressing FBXL2 (Figure S3).

Finally, we further validated these findings in Huh-7.5 cells infected with either wild-type Jc1FLAG2(p7-nsGLuc2A) or its BMS-790052-resistant version, containing an F28S substitution in the NS5A protein (Fridell et al., 2011). In agreement to the above results, BMS-790052 induced IP3R3 accumulation and impaired the binding of FBXL2 to both wild-type NS5A and IP3R3 (Figure 4D). In contrast, neither reduced binding of NS5A to FBXL2 nor accumulation of IP3R3 was seen in cells infected with the BMS-790052-resistant virus (Figure 4D).

Taken together, these results indicate that delocalization of NS5A from ER membranes impairs the ability of NS5A to promote FBXL2 binding to IP3R3 and the consequent IP3R3 degradation.

DISCUSSION

When cells are stimulated to produce IP_3, IP3R3 allows rapid mobilization of Ca^{2+} from the ER to mitochondria. To avoid excessive and prolonged flux of Ca^{2+} and prevent apoptosis, IP3R3 is degraded via SCF^{FBXL2} in a process that requires proper localization of FBXL2 (Kuchay et al., 2017).

HCV infection affects millions of people worldwide (Lindenbach and Rice, 2005; Rice and Saeed, 2014). HCV primarily infects hepatocytes, where it develops intricate relationships with a large number of cellular proteins to establish replication. Perturbation of protein geranylgeranylation results in the inhibition of HCV replication (Kapadia and Chisari, 2005; Ye et al., 2003). The absence of prenylation motifs in HCV proteins suggests that one or more geranylgeranylated host proteins promote HCV replication. FBXL2 was identified in a screen of host geranylgeranylated proteins required for efficient HCV replication and shown to interact with the HCV protein NS5A (Wang et al., 2005). In the absence of HCV infection, FBXL2 targets IP3R3 for degradation only after the cell is stimulated to produce IP_3, which unmasks the IP3R3 degron for accessibility to FBXL2 (Kuchay et al., 2017). Here, we show that NS5A allows IP3R3 recognition by FBXL2 in the absence of IP_3 induction by forming a trimeric complex that unmasks the degradation motif in IP3R3, resulting in IP3R3 degradation. Notably, the negative effect of FBXL2 silencing on HCV replication is rescued by IP3R3 depletion and, accordingly, expression of an FBXL2-insensitive, stable IP3R3 mutant inhibits HCV replication. Together, our results suggest that the FBXL2-NS5A-IP3R3 axis promotes HCV infection by enabling FBXL2 to target IP3R3 for degradation in a constitutive manner (i.e., in the absence of IP_3 stimulation), thus counteracting cell death.

We also found that the FBXL2(CaaX/SaaX), a geranylgeranylation-deficient mutant that fails to localize to cellular membranes (Kuchay et al., 2017; Wang et al., 2005), does not bind NS5A. Moreover, treatment with GGTI-286 results in the loss of binding between NS5A and FBXL2. Thus, geranylgeranylation of FBXL2 is necessary for its interaction with both IP3R3 and NS5A and for its ability to mediate IP3R3 degradation. Importantly, the GGTI-286-inhibited binding of FBXL2 to NS5A is rescued by expressing IP3R3(1–602), a mobile IP3R3 deletion mutant that is not at cellular membranes. These results suggest that, when FBXL2 and NS5A are delocalized, they do not interact because they are not in the same compartment with IP3R3. By contrast, IP3R3(1–602) allows this interaction because it is equally delocalized and can help bridging FBXL2 and NS5A. Thus, FBXL2 and NS5A can each independently bind IP3R3 (although this interaction is stabilized in the context of a trimeric complex). In contrast, the FBXL2-NS5A interaction appears to rely on the presence of IP3R3.

We used BMS-790052 as a tool to dislodge NS5A from ER membranes (Targett-Adams et al., 2011), where it interacts with FBXL2, and test how it affects the NS5A-FBXL2-IP3R3 complex formation. We show that, in both HCV-infected cells and HCV subgenomic replicons, BMS-790052 inhibits FBXL2 binding to both NS5A and IP3R3 and induces IP3R3 stabilization. Significantly, BMS-790052 has no effect on FBXL2 binding and IP3R3 stabilization in cells infected with the BMS-790052-resistant HCV mutant. Thus, inhibiting ER membrane localization of either NS5A (by BMS-790052) or FBXL2 (by GGTI-286) inhibits FBXL2-NS5A-IP3R3 interaction.

We propose a two-step model: in the first step, NS5A binds IP3R3 and unmasks its degron, and in the second, FBXL2 is recruited to target IP3R3 for degradation. This event prevents an IP3R3-mediated apoptotic response to HCV infection, allowing longer periods of viral replication and persistence.

STAR★METHODS

Detailed methods are provided in the online version of this paper and include the following:

- KEY RESOURCES TABLE
- CONTACT FOR REAGENT AND RESOURCE SHARING
- EXPERIMENTAL MODEL AND SUBJECT DETAILS
- METHOD DETAILS
  - Mitochondrial calcium measurements by Aequorin
  - Ubiquitylation assay
  - HCV replication assay
  - Detection of apoptosis and cell viability
  - Cells culture and transfection
- QUANTIFICATION AND STATISTICAL ANALYSIS
- DATA AND SOFTWARE AVAILABILITY

SUPPLEMENTAL INFORMATION

Supplemental Information includes three figures and one table and can be found with this article online at https://doi.org/10.1016/j.celrep.2018.09.088.

ACKNOWLEDGMENTS

The authors thank C. Espirit and E. Schenkein for their contribution to this study. M.P. is grateful to T.M. Thor for continuous support. This work was funded by grants from the NIH to M.P. and C.M.R., a Helmsley Postdoctoral Fellowship for Basic and Translational Research at The Rockefeller University to M.S., and grants from AIRC, funds from Ferrara's University (5x1000), and the Italian Ministry of Health and Cariplo to C.G. and P.P. M.P. is an Investigator with the Howard Hughes Medical Institute.

AUTHOR CONTRIBUTIONS

S.K. and M.S. performed co-designed all experiments and helped to write the manuscript. M.P. directed and coordinated the study, co-designed most experiments, oversaw all results, and co-wrote the manuscript. C.M.R. supervised the study. J.L. helped with the generation of some reagents. C.G. and P.P. performed the calcium-related experiments. All authors discussed the results and commented on the manuscript.

DECLARATION OF INTERESTS

M.P. is a member of the scientific advisory board of Kymera Therapeutics (previously known as Project Chimera, Inc.), Cambridge, MA and CullGen, Inc., San Diego, CA. He is also a consultant for BeyondSpring Pharmaceuticals, LLC, NYC, NY. S.K. consulted for BeyondSpring Pharmaceuticals, LLC, NYC, NY.

Received: March 23, 2018
Revised: July 17, 2018
Accepted: September 26, 2018
Published: October 23, 2018

REFERENCES

Blackshaw, S., Sawa, A., Sharp, A.H., Ross, C.A., Snyder, S.H., and Khan, A.A. (2000). Type 3 inositol 1,4,5-trisphosphate receptor modulates cell death. FASEB J. *14*, 1375–1379.

Blight, K.J., McKeating, J.A., and Rice, C.M. (2002). Highly permissive cell lines for subgenomic and genomic hepatitis C virus RNA replication. J. Virol. *76*, 13001–13014.

Bonora, M., Giorgi, C., Bononi, A., Marchi, S., Patergnani, S., Rimessi, A., Rizzuto, R., and Pinton, P. (2013). Subcellular calcium measurements in mammalian cells using jellyfish photoprotein aequorin-based probes. Nat. Protoc. *8*, 2105–2118.

Bourlière, M., Gordon, S.C., Flamm, S.L., Cooper, C.L., Ramji, A., Tong, M., Ravendhran, N., Vierling, J.M., Tran, T.T., Pianko, S., et al.; POLARIS-1 and POLARIS-4 Investigators (2017). Sofosbuvir, velpatasvir, and voxilaprevir for previously treated HCV infection. N. Engl. J. Med. *376*, 2134–2146.

Dankert, J.F., Rona, G., Clijsters, L., Geter, P., Skaar, J.R., Bermudez-Hernandez, K., Sassani, E., Fenyö, D., Ueberheide, B., Schneider, R., and Pagano, M. (2016). Cyclin F-mediated degradation of SLBP limits H2A.X accumulation and apoptosis upon genotoxic stress in G2. Mol. Cell *64*, 507–519.

Fan, G., Baker, M.L., Wang, Z., Baker, M.R., Sinyagovskiy, P.A., Chiu, W., Ludtke, S.J., and Serysheva, I.I. (2015). Gating machinery of InsP3R channels revealed by electron cryomicroscopy. Nature *527*, 336–341.

Fridell, R.A., Qiu, D., Valera, L., Wang, C., Rose, R.E., and Gao, M. (2011). Distinct functions of NS5A in hepatitis C virus RNA replication uncovered by studies with the NS5A inhibitor BMS-790052. J. Virol. *85*, 7312–7320.

Giorgi, C., De Stefani, D., Bononi, A., Rizzuto, R., and Pinton, P. (2009). Structural and functional link between the mitochondrial network and the endoplasmic reticulum. Int. J. Biochem. Cell Biol. *41*, 1817–1827.

Giorgi, C., Baldassari, F., Bononi, A., Bonora, M., De Marchi, E., Marchi, S., Missiroli, S., Patergnani, S., Rimessi, A., Suski, J.M., et al. (2012). Mitochondrial Ca(2+) and apoptosis. Cell Calcium *52*, 36–43.

Kapadia, S.B., and Chisari, F.V. (2005). Hepatitis C virus RNA replication is regulated by host geranylgeranylation and fatty acids. Proc. Natl. Acad. Sci. USA *102*, 2561–2566.

Kuchay, S., Duan, S., Schenkein, E., Peschiaroli, A., Saraf, A., Florens, L., Washburn, M.P., and Pagano, M. (2013). FBXL2- and PTPL1-mediated degradation of p110-free p85β regulatory subunit controls the PI(3)K signalling cascade. Nat. Cell Biol. *15*, 472–480.

Kuchay, S., Giorgi, C., Simoneschi, D., Pagan, J., Missiroli, S., Saraf, A., Florens, L., Washburn, M.P., Collazo-Lorduy, A., Castillo-Martin, M., et al. (2017). PTEN counteracts FBXL2 to promote IP3R3- and Ca^{2+}-mediated apoptosis limiting tumour growth. Nature *546*, 554–558.

Lindenbach, B.D., and Rice, C.M. (2005). Unravelling hepatitis C virus replication from genome to function. Nature *436*, 933–938.

Liu, D., Ji, J., Ndongwe, T.P., Michailidis, E., Rice, C.M., Ralston, R., and Sarafianos, S.G. (2015). Fast hepatitis C virus RNA elimination and NS5A redistribution by NS5A inhibitors studied by a multiplex assay approach. Antimicrob. Agents Chemother. *59*, 3482–3492.

Marukian, S., Jones, C.T., Andrus, L., Evans, M.J., Ritola, K.D., Charles, E.D., Rice, C.M., and Dustin, L.B. (2008). Cell culture-produced hepatitis C virus does not infect peripheral blood mononuclear cells. Hepatology *48*, 1843–1850.

Mattson, M.P., and Chan, S.L. (2003). Calcium orchestrates apoptosis. Nat. Cell Biol. *5*, 1041–1043.

Orrenius, S., Zhivotovsky, B., and Nicotera, P. (2003). Regulation of cell death: the calcium-apoptosis link. Nat. Rev. Mol. Cell Biol. *4*, 552–565.

Rice, C.M., and Saeed, M. (2014). Hepatitis C: treatment triumphs. Nature *510*, 43–44.

Saeed, M., Scheel, T.K., Gottwein, J.M., Marukian, S., Dustin, L.B., Bukh, J., and Rice, C.M. (2012). Efficient replication of genotype 3a and 4a hepatitis C virus replicons in human hepatoma cells. Antimicrob. Agents Chemother *56*, 5365–5373.

Skaar, J.R., Pagan, J.K., and Pagano, M. (2009). SnapShot: F box proteins I. Cell *137*, 1160–1160.e1.

Skaar, J.R., Pagan, J.K., and Pagano, M. (2013). Mechanisms and function of substrate recruitment by F-box proteins. Nat. Rev. Mol. Cell Biol. *14*, 369–381.

Targett-Adams, P., Graham, E.J., Middleton, J., Palmer, A., Shaw, S.M., Lavender, H., Brain, P., Tran, T.D., Jones, L.H., Wakenhut, F., et al. (2011). Small molecules targeting hepatitis C virus-encoded NS5A cause subcellular redistribution of their target: insights into compound modes of action. J. Virol. *85*, 6353–6368.

Wang, C., Gale, M., Jr., Keller, B.C., Huang, H., Brown, M.S., Goldstein, J.L., and Ye, J. (2005). Identification of FBL2 as a geranylgeranylated cellular protein required for hepatitis C virus RNA replication. Mol. Cell *18*, 425–434.

Wose Kinge, C.N., Espiritu, C., Prabdial-Sing, N., Sithebe, N.P., Saeed, M., and Rice, C.M. (2014). Hepatitis C virus genotype 5a subgenomic replicons for evaluation of direct-acting antiviral agents. Antimicrob. Agents Chemother *58*, 5386–5394.

Ye, J., Wang, C., Sumpter, R., Jr., Brown, M.S., Goldstein, J.L., and Gale, M., Jr. (2003). Disruption of hepatitis C virus RNA replication through inhibition of host protein geranylgeranylation. Proc. Natl. Acad. Sci. USA *100*, 15865–15870.

STAR★METHODS

KEY RESOURCES TABLE

REAGENT or RESOURCE	SOURCE	IDENTIFIER
Antibodies		
FBXL2 (1: 200 dilution)	Michele Pagano Lab Yenzyme customer ab	N/A
NS5A (1:1000 dilution)	Charlie Rice Lab	9E10
IP3R3 (1:1000 dilution)	BD Biosciences	Cat# 610312; RRID:AB_397704
GFP (1:1000 dilution)	Cell Signaling Technology	Cat# 2956; RRID:AB_1196615
FLAG (1:1,000 dilution)	Sigma-Aldrich	Cat# F7425; RRID:AB_439687
HA (1:1,000 dilution)	Covance	Cat# MMS-101P; RRID:AB_10064068
CUL1 (1:1,000 dilution)	Life Technologies	Cat# 322400
SKP1 (1:1,000 dilution)	Michele Pagano Lab Yenzyme customer ab	N/A
cleaved PARP (1:1000 dilution)	Cell Signaling Technology	Cat# 5625S; RRID:AB_10699459
Caspase 3 (1:1,000 dilution)	Cell Signaling Technology	Cat# 9662S; RRID:AB_10694681
Cleaved caspase-3 (1:1,000 dilution)	Cell Signaling Technology	Cat# 9661S; RRID:AB_2341188
Actin (1:10,000 dilution)	Sigma-Aldrich	Cat# A5441; RRID:AB_476744
Tubulin (1:10,000 dilution)	Sigma-Aldrich	Cat# T6074; RRID:AB_477582
Chemicals, Peptides, and Recombinant Proteins		
GGTI-286	Millipore	Cat# 345878
BMS-790052,	Selleck Chemicals	Cat# S1482
MG132 (final concentration, 5 mM)	Peptide international	Cat# IZL-3175v
Hydrogen peroxide solution	Sigma-Aldrich	Cat# H1009
VFSNNDEGLINKKC (FBXL2 peptide to generate antibody)	Michele Pagano Lab	Yenzyme
x-tremeGENE HP transfection	Roche	Cat# 06366236001
HiPerfect™	QIAGEN	Cat# 301704
M2-FLAG Affinity Matrix	Sigma-Aldrich	Cat # A2220
Anti-HA Affinity Matrix	Roche	Cat# 11815016001
Anti-GFP (Green Fluorescent Protein) mAb-Agarose	MBL International	Cat# D153-8
Lipofectamine RNAiMAX Transfection Reagent	ThermoFisher Scientific	Cat# 13778150
Lipofectamine 3000 Transfection Reagent	ThermoFisher Scientific	Cat# L3000015
Deposited Data		
Raw data	this paper	https://data.mendeley.com/datasets/9x346zd8bx/draft?a=1d6f03e8-7016-437e-a3ef-34fc00ba474b
Experimental Models: Cell Lines		
HEK293T	ATCC	Cat# CRL-3216
NHF	ATCC	Cat# CCL-186
HepG2	ATCC	Cat# HB-8065
COS-7	ATCC	Cat# CRL-1615
HeLa	ATCC	Cat# CCL-2
Huh7.5	Charlie Rice Lab (Blight et al., 2002)	N/A
Huh7.5-JFH1	Charlie Rice Lab (Saeed et al., 2012)	N/A
Huh7.5- Con1	Charlie Rice Lab (Wose Kinge et al., 2014)	N/A

(*Continued on next page*)

Continued

REAGENT or RESOURCE	SOURCE	IDENTIFIER
Critical Commercial Assays		
TiterTACS™ TUNEL assays	TREVIGEN	Cat# 4822-96-k
Luciferase Assay System	Promega	Cat# E1500
Oligonucleotides		
siRNAs to FBXL2	Dharmacon (Kuchay et al., 2017)	N/A
siRNAs to IP3R3	Dharmacon (Kuchay et al., 2017)	N/A
siRNAs to MCU	Dharmacon (Kuchay et al., 2017)	N/A
siRNAs to p85β	Dharmacon (Kuchay et al., 2017)	N/A
Non-targeting siRNA (CGUACGCGGAAUACUUCGA)	Dharmacon (Kuchay et al., 2017)	N/A
RPS11 primer_Forward 5′-GCC GAG ACT ATC TGC ACT AC-3′,	Integrated DNA Technology, USA	N/A
RPS11 primer_Reverse 5′-ATG TCC AGC CTC AGA ACT TC-3′	Integrated DNA Technology, USA	N/A

CONTACT FOR REAGENT AND RESOURCE SHARING

Request for resources and reagents should be directed to Lead Contact, Michele Pagano (Michele.Pagano@nyulangone.org).

EXPERIMENTAL MODEL AND SUBJECT DETAILS

Experiments were performed either in cell lines purchased from ATCC (HEK293T, NHF, HepG2, COS-7, HeLa) or in Huh7.5 cells bearing non-infectious HCV replicons (described in the Key Resource Table). These cell lines were not authenticated.

METHOD DETAILS

Mitochondrial calcium measurements by Aequorin

Cells were grown on 13 mm round glass coverslips at 50% confluence, and were transfected with mtAEQ (a bioluminescent calcium sensor aequorin chimera which contains a sequence specifically targeting it to mitochondria) either alone or together with constructs expressing GFP-IP3R3, GFP-IP3R3(Q-FR/A-AA) and FLAG-NS5A as indicated in figure legends. Mitochondrial calcium measurements with mtAEQ were carried out, as previously described (Kuchay et al., 2017), in KRB buffer (125 mM NaCl, 5 mM KCl, 1 mM $MgSO_4$, 1 mM Na_2HPO_4, 5.5 mM glucose, 20 mM $NaHCO_3$, 2 mM l-glutamine and 20 mM HEPES pH 7.4, and was supplemented with 1 mM $CaCl_2$). Agonists and other drugs were added to the same medium, as specified in the figure legends. The experiments were terminated by lysing cells with 100 μM digitonin in a hypotonic Ca^{2+}-rich solution (10 mM $CaCl_2$ in H_2O), thus discharging the remaining aequorin pool. The light signal was collected and calibrated into $[Ca^{2+}]$ values, as previously described (Bonora et al., 2013).

Ubiquitylation assay

Huh7.5 cells were transiently transfected with FLAG-tagged trypsin-resistant tandem ubiquitin-binding entity (TR-TUBE), which directly binds polyubiquitin chains and protects them from proteasome-mediated degradation. Six hours after transfection, cells were either left uninfected or infected with Jc1FLAG2(p7-nsGLuc2A), a highly infectious HCVcc virus. 48 hours post-infection cells were harvested and whole cell lysates of infected and uninfected cells were used for immunoprecipitations with anti-FLAG M2 agarose beads (Sigma) as previously described (Dankert et al., 2016; Kuchay et al., 2017). Immunoprecipitated complexes were boiled for 10 minutes, subjected to SDS-PAGE and western blotting with antibodies specified in the figures. Polyubiquitinated IP3R3 was detected with an IP3R3 antibody.

HCV replication assay

Huh7.5-JFH1 and Huh7.5-Con1 cells are cell lines harboring persistently replicating HCV subgenomic replicons from genotype 2a (JFH1/SG-Feo) and genotype 1b (Con1/SG-Feo S2204I), respectively. The replicons express a fusion protein of firefly luciferase (Fluc) and neomycin phosphotransferase II (NPTII), permitting selection of the replicon carrying cells and measurement of the levels of HCV replication. For HCV RNA replication assays, cells were seeded in 24 well plates at a density of 0.5-1 $x10^5$cells/well. For knockdown experiments, two rounds of siRNA transfection, one at 24 hours and the other at 48 hours post-cell seeding, were performed using HiPerfect transfection reagent. The final concentration of siRNA in each well was 20 nM. Four hours after second transfection, cells were trypsinized and re-plated in new 24-well plates where they were grown for another 48 hours before measurement

of FLuc activity. For gene overexpression, cells were transfected with 1 μg DNA/well for 12-14 hours using x-tremeGENE HP transfection reagent. Cells were trypsinized, and re-plated in fresh 24 well plates where they were grown for additional 48 hours before lysis and Fluc assay. Cell lysates for FLuc assay were prepared with 1X Cell Culture Lysis Reagent (Promega) and luciferase activity was measured with the Luciferase Assay System (Promega) using an Infinite® M200 PRO multimode microplate reader (TECAN). For HCV infection assay, Huh-7.5 cells were seeded in 24-well plates at a density of $7.5X10^4$ cells/well. Two rounds of siRNA transfection were carried out 24 hours apart, similar to the replicon cells. Twenty four hours after second round of transfection, cells were infected with Jc1FLAG2(p7-nsGLuc2A), a highly infectious HCVcc virus (Marukian et al., 2008). Four hours later, cell monolayer was washed 3X with PBS to remove luciferase protein contained in the HCVcc stock and a fresh medium was added to each well. Cells were grown for 48 hours, before the culture medium was harvested and HCV RNA replication level was monitored by the measurement of secreted gaussia luciferase. For immunoblotting, infected and non-infected cells were trypsinized, washed with PBS and cell pellets were frozen on dry ice. Whole cell lysates were prepared for SDS-PAGE and western blotting with antibodies specified in figures.

Detection of apoptosis and cell viability

Cells were treated with apoptotic stimuli, as specified in the figure legends, in DMEM supplemented with 10% FBS for cell death induction, as indicated in the text and figure legends. Apoptosis was determined by (i) by blotting for different cell death markers, such as cleaved PARP, Caspase 3 and cleaved Caspase-3; (ii) TiterTACS™ TUNEL assays in JFH1 and Con1 cells, transiently transfected with empty vector (EV), GFP-IP3R3, or GFP_IP3R3(Q-FR/A-AA), performed in 96 well format (0.5-1 × 10^4cell/well) according to manufactures protocol (TREVIGEN). Cell viability was evaluated by automated nuclei count analysis from randomly chosen fields, specified in figure legends, using Zeiss Axiovert 200M microscope as described previously (Kuchay et al., 2017).

Cells culture and transfection

NHFs and cell lines (HEK293T, COS-7, HeLa) were purchased from ATCC and maintained as previously described (Kuchay et al., 2017). Huh-7.5 cells were grown in DMEM supplemented with 10% fetal bovine serum and 0.1 mM non-essential amino acids (NEAA). G418 was added to the medium at a concentration of 750 μg/mL to select and maintain Huh7.5-JFH1 and Huh7.5-con1 cells carrying HCV subgenomic replicons from genotype 2a (JFH1/SG-Feo) and genotype 1b (Con1/SG-Feo S2204I), respectively. JFH1/SG-Feo replicons are described (Saeed et al., 2012). Con1/SG-Feo S2204I replicon was made from full-length Con1 cDNA following the same method described for JFH1/SG-Feo and a cell culture-adaptive mutation S2204I, a substitution of serine at position 2204 with isoleucine, was introduced to increase the replication level (Blight et al., 2002). HeLa, HepG2 and COS-7 cells (African Green Monkey SV40-transformed kidney fibroblasts) were grown in DMEM supplemented with 10% FBS and transfected with a standard calcium-phosphate procedure. Cells were serum-starved in DMEM 0.1% FBS (HeLa and COS-7 for 20 hours, NHFs for 48-72 hours) and then serum stimulated with 10% FBS containing DMEM for the indicated times. For gene silencing, cells were seeded 24 hours before transfection. ON TARGET siRNA oligos from Dharmacon, Inc. for FBXL2, p85β, IP3R3, MCUa and non-targeting controls (5 nM) were used in serum free medium for 24-48 hours using HiPerfect™, according to the manufacturer's instruction (QIAGEN) as previously described (Kuchay et al., 2017). IP3R3, PIK3R2 and FBXL2 silencing, and FBXL2 mRNA quantification was carried out as described previously (Kuchay et al., 2017). Details for the RPS11 primer sequences used as housekeeping control for FBXL2 mRNA quantification are provided in KEY RESOURCES TABLE.

QUANTIFICATION AND STATISTICAL ANALYSIS

Figure legends include the specific statistical details. Statistical data are presented as mean ± SD and ± SEM and significance were calculated by Student's t tests, and correlation analysis was done by ANOVA using the Graphpad prism software. All data used for the statistical analysis in main and supplemental figures are listed in Table S1.

DATA AND SOFTWARE AVAILABILITY

Raw data was deposited in Mendeley at https://data.mendeley.com/datasets/9x346zd8bx/draft?a=1d6f03e8-7016-437e-a3ef-34fc00ba474b.